Cyanines Substituted on Heptamethine Chain and their Conjugates as Fluorescent Labels

Rebecca Strada,[1,*] Zdeněk Farka,[2] Peter Šebej[1]

[1]RECETOX and [2] Dept. of Biochemistry, Faculty of Science, Masaryk University, Kamenice 753/5, 625 00 Brno, Czech Republic

E-mail: rebecca.strada@recetox.muni.cz

MUNI | RECETOX

Noninvasive **imaging with visible/NIR light** represents an **intriguing tool for extracting biological information** from cells, tissues, and living subjects. While light in the visible range is routinely used for intravital microscopy, imaging of deeper tissues (> 500 μm up to 1 cm) requires the use of near infra-red (NIR) light. Hemoglobin and water, the major absorbers of visible and infrared light, respectively, have their lowest absorption coefficient in the far-red and NIR region around 600-900 nm,[1] called **tissue transparent window** (TTW).

Near infra-red fluorescence emission imaging is widely used in tracking biological processes and disease diagnosis due to its non-invasive, real-time and multi-dimensional monitoring characteristics.

There is only one NIR emitting dye approved by the FDA, EMA and other regulatory bodies for use in human diagnosis, indocyanine green (ICG)[6] and one in later stage of pipeline of clinical trials, IRDye 800CW.[7] Both belong to the cyanine family of dyes, a subgroup of polymethine chromophores.

The structure of generic cyanine consists of two nitrogen heterocycles, linked by a conjugated polymethine chain with an odd number of carbon atoms. They represent a wide and versatile family of fluorophores with three key points allowing tuning of their properties: (a) the length of the polymethine chain, (b) the end-substituents and (c) the substitution of polymethine chain itself.

The aim of our work is to investigate the behavior of newly-synthesized polymethine dyes with potentially increased stability, brightness and/or red-shifted absorption and emission.

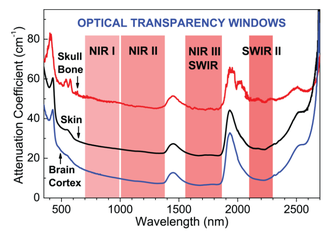

Fig. 1 Spectra of attenuation coefficient for head tissues. Four optical transparency windows are indicated: 700-1000 nm (NIR-I), 1000-1350 nm (NIR-II), 1550-1870 nm (NIR-III or SWIR) and 2100-2300 nm (SWIR-II)[8].

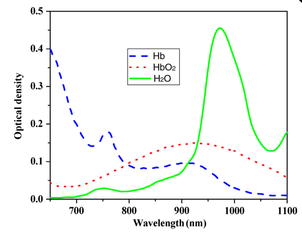

Fig. 2 Absorption spectra of deoxyhemoglobin (Hb), hemoglobin (HbO_2) and water in the visible and NIR region[9].

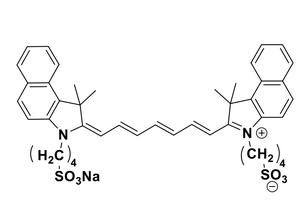

Indocyanine green (ICG)

λ_{abs} = 785 nm λ_{em} = 815 nm

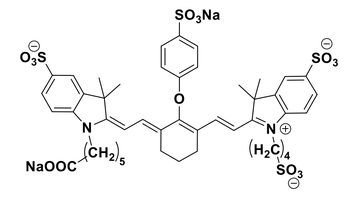

IRDye 800CW

λ_{abs} = 767 nm λ_{em} = 786 nm

I. Synthesis of Heptamethine Dyes

A newly-established strategy involving the ring opening of pyridinium salts (Zincke salts) and subsequent incorporation of the original substituted pyridine residue (red) into the heptamethine chain[3].

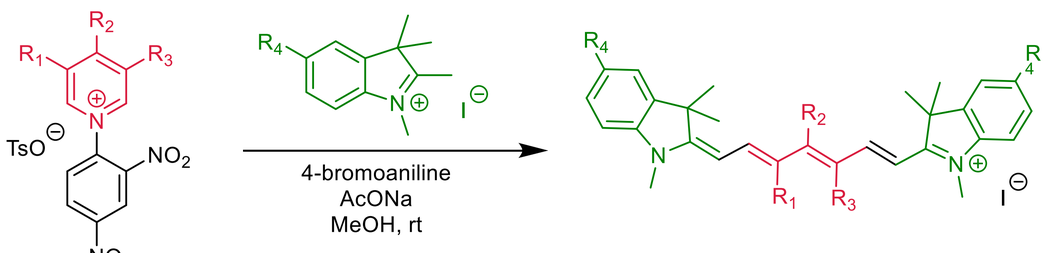

EWD and EDG functional groups were attached on the heterocyclic ring, followed by the investigation of their effects on the photophysical properties and bioconjugation. Our studies suggested that the type of functional group on the indolenine ring slightly influences the photophysical properties.

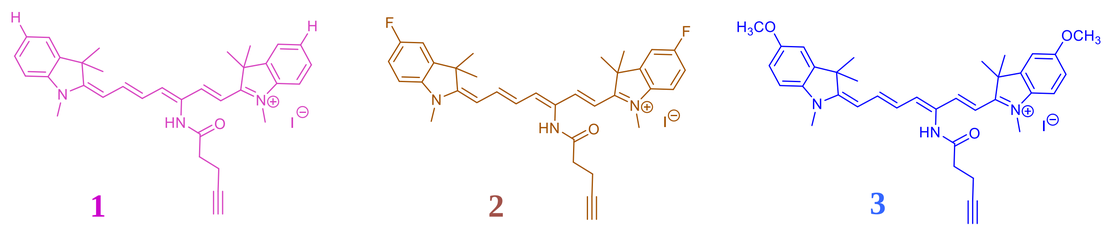

II. Photophysical Properties

Cyanine	Solvent	λ_{max}(abs)/nm	log ε^b	λ_{max}(ems)/nm	Φ_f	$\varepsilon\Phi/10^{3.c}$
1	CH_3OH^a	735	5.31	765	0.084±0.001	17.2
	PBS[f]	729	5.25	754	0.055±0.002	9.8
2	CH_3OH	735	5.52	765	0.084±0.002	27.9
	PBS	730	5.38	756	0.049±0.006	11.8
3	CH_3OH	760	4.95	789	0.028±0.005	2.5
	PBS	747	4.77	777	0.017±0.005	1.0
ICG[d]	CH_3OH	779	n.d.[e]	807	0.12	n.d.
	H_2O	785	n.d.	815	0.0028	n.d.

[a] Solutions in methanol: $A(\lambda_{max}) \approx 1$ ($c = 2 - 8 \times 10^{-5}$ mol dm^{-3}) was adjusted for absorption spectroscopy, and $A(\lambda_{max}) < 0.1$ ($c < 2 \times 10^{-5}$ mol dm^{-3}) was used for emission spectroscopy and fluorescence quantum yield measurements; all experiments were performed at 22 °C. [b] log [ε/mol dm^{-3} cm^{-1}]. [c] $\varepsilon\Phi/10^3$ mol dm^{-3} cm^{-1}; fluorophore brightness (the product of the molar absorption coefficient at λ_{em}^{max} and the corresponding fluorescence quantum yield. [d] Data from ref.[6,]. [e] Not determined. [f] Measured in aqueous PBS (1×) solution containing 1% DMSO (*v*/*v*) as a co-solvent.

Absorption and emission spectra measured in CH_3OH

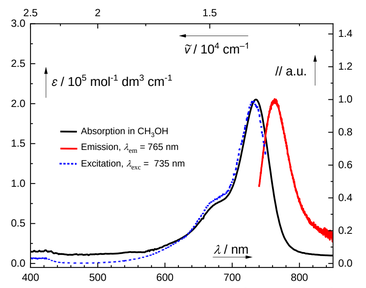

Dye 1. UV-Vis Absorption and Normalized Fluorescence Emission (CH_3OH, A (λ_{max}) < 0.1, $c \sim 3.45 \times 10^{-6}$ mol dm^{-3})

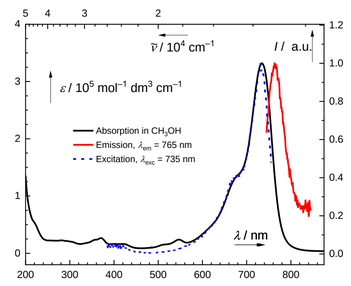

Dye 2. UV-Vis Absorption and Normalized Fluorescence Emission (CH_3OH, A (λ_{max}) < 0.1, $c \sim 4.5 \times 10^{-5}$ mol dm^{-3})

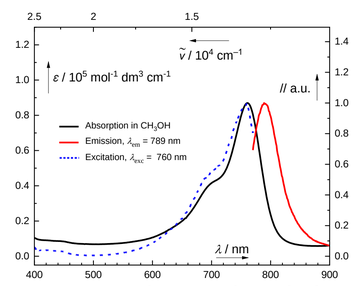

Dye 3. UV-Vis Absorption and Normalized Fluorescence Emission (CH_3OH, A (λ_{max}) < 0.1, $c \sim 7.0 \times 10^{-5}$ mol dm^{-3})

Absorption and emission spectra measured in PBS with 1% DMSO (*v*/*v*) as co-solvent

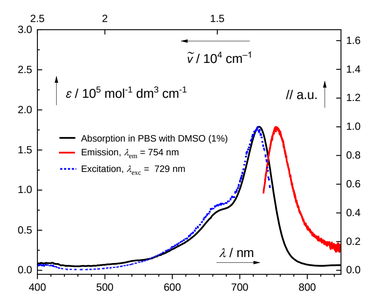

Dye 1. UV-Vis Absorption and Normalized Fluorescence Emission (PBS with 1% DMSO, A (λ_{max}) < 0.1, $c \sim 6.34 \times 10^{-5}$ mol dm^{-3})

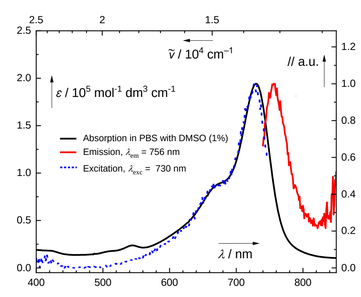

Dye 2. UV-Vis Absorption and Normalized Fluorescence Emission (PBS with 1% DMSO, A (λ_{max}) < 0.1, $c \sim 4.5 \times 10^{-5}$ mol dm^{-3})

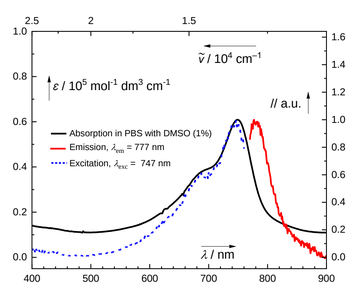

Dye 3. UV-Vis Absorption and Normalized Fluorescence Emission (PBS with 1% DMSO, A (λ_{max}) < 0.1, $c \sim 5.0 \times 10^{-5}$ mol dm^{-3})

Kinetic studies of the dark decomposition in PBS + 1% DMSO (*v*/*v*) showed that the half-life of **1** and **2** is $t_{1/2} \sim 4$ days while for **3** $t_{1/2} \sim 2$ days

III. Bioconjugation

The bioconjugation was performed using the Copper(I)-catalyzed Azide-Alkyne Cycloaddition[4], CuAAC.

Azides and alkynes are particularly useful because they are small, unobtrusive and unlikely to perturb the biological molecules to which they are attached.

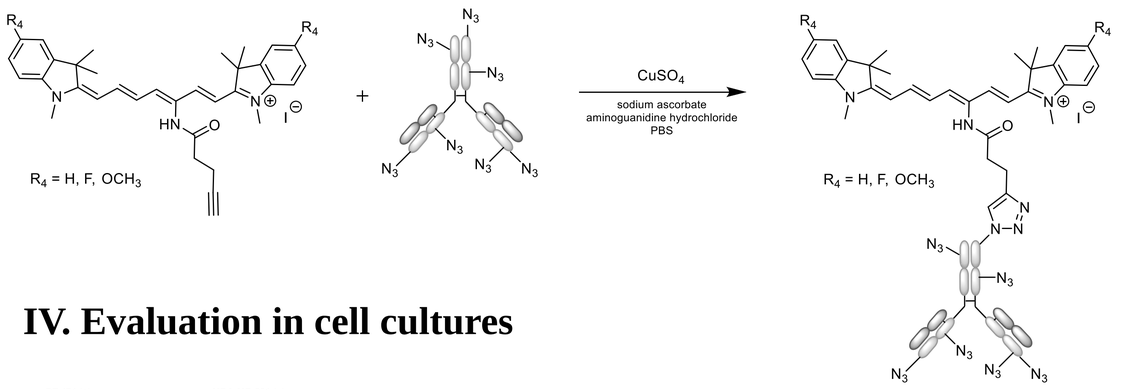

IV. Evaluation in cell cultures

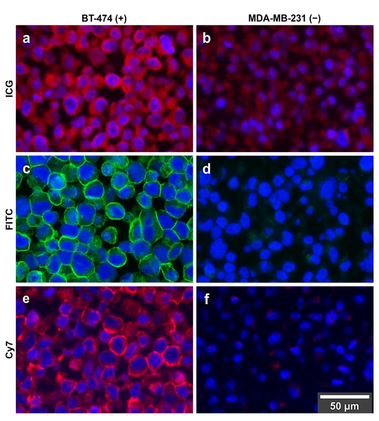

Immunofluorescence detection of HER2 on breast cancer cell lines (HER2-positive on left panels; HER2-negative on the right panels).

a, b) anti-rabbit antibody conjugate with ICG
c, d) anti-rabbit antibody conjugate with fluorescein (from FITC)
e, f) anti-rabbit antibody conjugate with Cy7

Red channel corresponds to ICG/Cy7; green channel corresponds to fluorescein; blue channel represents DAPI stained cellular nuclei.

V. Conclusions

The synthesized dyes shows slightly differences in their photophysical properties. Further studies will be focused on the synthesis and photophysical characterization of new dyes.

VI. References

1. Weissleder, R. Nat. Biotechnol., 2001, 19, 316–317.
2. Escobedo, J. O.; Rusin, O.; Lim, S.; Strongin, R. M. Curr. Opin. Chem. Biol., 2010, 14 (1), 64–70.
3. Šťacková, L.; Muchová, E.; Russo, M.; Slavíček, P.; Štacko, P.; Klán, P. J. Org. Chem., 2020, 85 (15), 9776–9790.
4. Presolski, S. I.; Hong, V. P.; Finn, M. G. Curr. Protoc. Chem. Biol., 2011, 3 (4), 153–162.
5. Carr, J. A. et al. Proc. Natl. Acad. Sci., 2018, 201718917.
6. Desmettre, T.; Devoisselle, J. M.; Mordon, S. Surv. Ophthalmol., 2000, 45 (1), 15–27.
7. Gorka, A. P.; Nani, R. R.; Schnermann, M. J. Acc. Chem. Res., 2018, 51 (12), 3226–3235.
8. Golovynskyi, S.; Golovynska, I.; Stepanova, L. I.; Datsenko, O. I.; Liu, L.; Qu, J.; Ohulchanskyy, T. Y. J. Biophotonics, 2018, 11 (12).
9. Sordillo, L. A.; Pu, Y.; Pratavieira, S.; Budansky, Y.; Alfano, R. R. J. Biomed. Opt., 2014, 19 (5).

Acknowledgment

This work was supported by the Czech Science Foundation (GJ20-30004Y), CETOCOEN EXCELLENCE Teaming 2 (CZ.02.1.01/0.0/0.0/17_043/0009632), and RECETOX RI (LM2018121)